# Distribution and migration of shallow-water hake (*Merluccius capensis*) in the Benguela Current Large Marine Ecosystem examined with a geostatistical population model – a preview *

Teunis Jansen[1,5], Kasper Kristensen[5], Uffe Høgsbro Thygesen[5] and Jan E. Beyer[5]

1) BCC – Benguela Current Commission, Private Bag 5031, Swakopmund, Namibia.
2) MFMR – Ministry of Fisheries and Marine Resources, PO Box 912, Swakopmund, Namibia.
3) DAFF – Department for Agriculture, Forestry & Fisheries, Cape Town, South Africa.
4) Institute of Marine Research, P.O. Box 1870 Nordnes, N-5817 Bergen, Norway.
5) DTU AQUA – National Institute of Aquatic Resources, Charlottenlund, Denmark
6) Department of Ichthyology and Fisheries Science, Rhodes University, P.O. Box 94, Grahamstown 6140 , South Africa

Corresponding author: Teunis Jansen; DTU AQUA - *National Institute of Aquatic Resources, Technical University of Denmark; Charlottenlund castle, 2920 Charlottenlund, Denmark; Tel.: +4530667840; Fax: +4533963333; E-mail address:* Tej@aqua.dtu.dk.

*** Disclaimer #1:** This study is *in progress.* The results are not final, so they should not be used outside the EcoFish phase II workshop.

*** Disclaimer #2:** Following scientists are contributing to this study: Paul Kainge[2], Deon Durholtz[3], Tore Strömme[4], Marek Lipinski[6], John Kathena[2], Margit Wilhelm[1,5], Tracey Fairweather[3], Sarah Paulus[2], Henrik Degel[5].

# Abstract

Shallow-water hake (*Merluccius capensis*) is of primary ecological and economic importance in the Benguela Current Ecosystem in South Africa and Namibia. The assessment and management is done under a series of assumptions about key aspects of the hake biology and behaviour, such as migration, population structure and growth. This information is imperative, if the resource is to be managed optimally.

For the first time, we combine data from the existing demersal trawl survey series to map and plot the distribution and migration of *M. capensis* for the entire Benguela large marine ecosystem. This reveals unknown aspects of the depth and alongshore migration patterns and how they differ between parts of the Benguela region. [Migration description to be added here]. The double-sided return migration demonstrated natal homing, but with unknown precision. Spatial population structures (sub-populations or stocks) may thus be persistent from generation to generation, or only be maintained during some phases of the hake life time. The stability over time as well as the level of mixing between these migration patterns and subpopulations needs to be further analyzed.

Our analyses were done with a new Latent Cohort GeoPop model – a geostatistical model (aggregated log Gaussian cox process model with correlations). This version tracks the cohorts in time and space. The spatial population structures and dynamics demonstrated herein, is a dimension of the hake population ecology that is not currently accounted for in stock assessment and management of one of the two most economically valuable fish resource in the region.

Keywords: *Hake, northern Benguela, southern Benguela, Merluccius capensis, transboundary, migration, geostatistics, LGC, growth, gear selectivity, South Africa, Namibia, demersal trawl, mortality*

# Introduction

Shallow-water cape hake (*Merluccius capensis*) is among the most dominant demersal fish species in the South East Atlantic. The species is ecologically important in the Benguela Current Large Marine Ecosystem as an opportunistic predator (mainly fish, including hake) (Botha, 1980; Payne et al., 1987), and as prey for the top predators such as fur seals, cephalopods, sea birds and many demersal and pelagic fish species (Pillar & Wilkinson, 1995). *M. capensis* (together with the sympatric deepwater hake *M.paradoxus*) is also targeted by fisheries throughout its distribution (BCC, 2012). Annual hake landings in Namibia, South Africa and Angola averaged 300,000 tonnes per year in 2000-2010, with over 70% being SWC hake (BCC, 2012). Hakes are the economically most important fish stocks in both Namibia and South Africa, worth about 5 % of the GDP in Namibia (MFMR & NPC, 2013).

*M. capensis* inhabit the continental shelf and upper slope from around 16°S in Angola to about 31°E in South Africa (Payne, 1989). Spawning mainly takes place between 50 and 200 meter depth on the continental shelf and shelf edge from South and West of South Africa to 20°S in Namibia (Jansen & et al., in prep). The spatial population structure (stock structure) remains uncertain and several hypotheses have been proposed. The area around the Lüderitz upwelling cell and Orange River Cone (LUCORC) region (25°-29°S) is believed to form a natural barrier between the northern Benguela and southern Benguela (e.g. Agenbag & Shannon, 1988; Duncombe Rae, 2005; Lett et al., 2007). Therefore, for the purposes of political simplicity, the national border between Namibia and South Africa (Orange River at 29 °S) has traditionally been regarded as the border dividing the species into two stocks (Figure 1) (Grant et al. 1987, 1988; Burmeister 2005). However, recent genetic analysis have questioned this perception of the population structure and suggested that SWC hake is panmictic (von der Heyden et al., 2007). Currently, management follow the old assumption of two stocks, but the possible need for transboundary management of the Cape hake stocks has been under discussion in recent years. Alongshore migration has been indicated for *M. capensis* in Namibian waters (Wilhelm, et al, Submitted), but is not known for South African waters. To date, no transboundary migration studies have been conducted. Offshore ontogentic migration to deeper water is documented (Botha, 1980; Burmeister, 2001; Gordoa & Duarte, 1991; Payne & Punt, 1995). Seasonal spawning migrations are believed to occur, but the paths and timing are unknown (BCC, 2012).

Nearly all studies of the biology and ecology of *M. capensis* have been on a local or national scale, even though several decades of high quality research survey data have been collected from demersal bottom trawl surveys throughout its entire distribution area. Regional transboundary analyses on the combined survey data sets (which only recently became available) have not been performed because the data are not directly comparable. The various surveys conducted by the three vessels have used different trawl gear with different catch efficiency. In the present study, we quantify this effect, so we can address the spatial population dynamics with a state-of-the-art integrated geostatistical population model. We develop a new version of the “GeoPop” model, which combines a novel geostatistical approach with a simple population model. The central aim of the study is to analyse the spatial population dynamics. We do this by estimating time series of cohort-specific distributions and map them for examination of putative migration patterns.

# Materials and methods

## *Scientific trawl survey data*

*M. capensis* were caught during demersal trawl surveys on the continental shelf and slope in the Benguela-Agulhas ecosystem from 17°S in the North, round Cape of Good Hope to 27°E in the west (Fig. 1). The surveys are conducted each year in January-May for routine biomass calculations by the Ministry of Fisheries and Marine Resources (MFMR) in Namibia and the Department of Agriculture Forestry and Fisheries (DAFF) in South Africa. No trawl samples were available from Angolan waters due to species identification problems between *M. capensis* and *M. paradoxus* and *M. polli* (Benguela hake, which is largely caught in Angola). Three different trawl gear types were used, each fishing at a different trawl speed or with different size spread or ropes (Table 1). Total catch was weighed and sorted by species. Large catches were subsampled. The weight of the hake catch (separated by species) was recorded and total lengths of individual hake were measured in cm (rounded down). Subsamples were subsequently raised to the total catch.

The standardized efficiency of the trawl was compromised by very strong winds in 2002 and 2011off the South African west coast (Wieland et al, in prep). These stations were therefore removed from the dataset.

Catch Per Unit Effort (CPUE) of each length group in each haul was calculated as number per hour trawled. This measure was used as a relative index of hake density.

The survey dataset consisted of 7.3 million measured *M. capensis* in 7,800 trawl hauls from 1998 to 2012. 510 of the hauls were especially informative in relation to gear inter-calibration, because they were taken with different gears, less than 3 hours apart and at a maximum distance of 18 nautical miles (nm). The samples were from the entire region (Figure 1), and they were fairly equally distributed among the years (Figure 2a). Most samples were taken in January-February, while the South African South coast was covered in April-May (Figure 2b). Trawling was predominantly done during the day (Figure 2c). The Gisund trawl was used most frequently (Figure 2d).

## *The Latent Cohort GeoPop model*

A geostatistical model (aggregated log Gaussian Cox process model with correlations) was used to describe the density index of *M. capensis* cohorts through space and time, along environmental gradients, observed using various gear types, as the hake recruited, grew and died.

Related models have previously proved their value for cod (Kristensen et al., 2013; Lewy & Kristensen, 2009) and mackerel larvae (Jansen et al., 2012). However, this new “Latent Cohort GeoPop model” tracks the cohorts. This is not only biologically meaningful, it is also advantageous for the complex and time consuming model fitting algorithm to reduce the number of parameters from 100 length classes to eight year classes. To obtain growth rates independent of otoliths-based age data, we integrated a length-frequency analysis (LFA) in the model complex. The LFA estimates the age distribution of a given length class by following the cohort-peaks in the length frequencies as they grow (Equation 2).

We modelled the density index (CPUE) for eight age classes in the period 1998 to 2012. The cohorts were followed in time steps of one year and in a spatial resolution of 25x25 km. These 135,120 (8 age classes x 15 years x 1126 grid-cells) random variables were assumed to follow a log Gaussian distribution, and determine the mean of catch (in numbers), which are assumed to follow a Poisson distribution, conditional on densities. This model structure is referred to as a log-Gaussian Cox process model, and has been shown as a good representation of count data from catches that are correlated, over-dispersed and with many zero-values (Kristensen et al., 2013). The Poisson distribution allows for zero catches, while the randomness of the density fields imply over-dispersed catches (relative to Poisson) and in particular many more zero catches than would be found in a pure Poisson model. Finally, the catches inherit the correlation structure of the density field.

A key feature of the model was the utilization of the information that resides in the patchy distribution of fish. This behavioural element was modelled in three parts: First and second, patchiness in space and in time on a large scale (correlations between cells) and, third, the tendency of fish to aggregate with fish in similar sizes on a local scale (within age groups, within trawl hauls, “nugget effect”).

The spatial large-scale correlation was assumed to decay with distance and the stability over time of these patterns was estimated as the correlation from year to year of the density in a given cell. Temporal correlation decayed exponentially with distance in time (years) and spatial correlation did approximately the same. However, in order to avoid correlation over land (e.g. the Cape point), we implemented the spatial correlation effect as a Gaussian Markov random field. To present the parameter estimates of these correlations in a meaningful way, we expressed the distance (*H*) and de-correlation time (*T*), as the distance in space and in time where the correlations have decayed to $e^{-1}$ (explaining approx. 14% of the variance). Documentation of these correlation structures were published in Kristensen et al. (2013).

The third relation in the model that should reflect fish behaviour was the “nugget effect”. Catches of certain fish sizes tend to be over-represented in trawl hauls compared to the size distribution in the sampled population. This may be due to size structured aggregations (schools) or because the local habitat favours fish of a certain size e.g. through the available type of food. This local effect was accounted for by estimating the age-class specific variation in the hauls ( $\sigma_N^2$ ).

A simple population model related the cohort abundance index from one year to the next, by estimating the mean recruitment ( $N_0$ ) and mean total mortality (*Z*). These processes were assumed to be independent of space and time. The mean total mortality was modelled as a constant corresponding to the exponential decay model:

$$N_t = N_0 e^{-\bar{Z}\Delta t} ,$$

where $N_t$ was the abundance after the mortality $\overline{Z}$ (year$^{-1}$) in $\Delta t$ time steps (in years)

We linked the observations by length to cohorts, by a size spectrum analysis. This part of the model followed the cohort signals as abundance peaks that grew up through the size spectrum. For simplicity, we assumed that the size distribution the individual fish in a cohort is given by a Gaussian density with a mean determined by a von Bertalanffy growth model:

$$L = L_{inf}(1 - e^{-K(a-t_0)}),$$

where $L$ is the mean length in cm at age class *a* (years), $L_{\mathrm{inf}}$ (cm) the mean length of infinitely old fish, i.e. the asymptotic length at which growth is theoretically zero, $K$ (Year$^{-1}$) is the rate at which $L$ approaches $L_{\mathrm{inf}}$ and $t_0$ (years) is the x-axis interception, i.e. a theoretical age at length 0 cm.

The standard deviation of the Gaussian distributed individual lengths around the mean length at age was assumed to increase linearly with age with $\sqrt{\sigma^2_{rate}}$ from the initial standard deviation $\sqrt{\sigma^2_{init}}$ .

The first cohort peak was assigned an age of 0.5 years, because the main spawning season lasts from July to September (centre assumed middle of August) (Kainge et al. 2007; Wilhelm et al., 2013; Jansen & et al., in prep) in the northern parts of the region, which were surveyed in January to February (centre assumed middle of January) (Jansen & et al., in prep). *M. capensis* off the South African south coast spawn about six months later (November–February, centre assumed middle of January) (Jansen & et al., in prep), where surveys take place later in the year (April-May, centre assumed middle of April).

Finally, the catch is affected by the catchability of the gear and this effect was implemented as

$$SF_G = \gamma(1 + 3^{-(2/SR_G)(l-L50_G)})^{-1} ,$$

where *SF* is the selection factor, $\gamma$ is the efficiency factor, *SR* is the selection range and L50 is the fish length (cm) at half selection for three different gear types *G*.

The parameters in the model were estimated using the maximum likelihood principle based on the Laplace approximation and thus the estimation follows the principles of Kristensen et al. (2013). However, the present model was more challenging due to non-convexity issues of the aggregated log Gaussian Cox process and the much larger area and amount of data - see details in Supplementary information 1. When possible, we followed the parameter notation of Kristensen et al. (2013). A more concise documentation of the present model was furthermore given in Supplementary information 2.

The fitted model was finally used to calculate annual estimates of the relative index of hake density (CPUE) for each cohort in each age class (0.5-7.5) in each 25 x 25 km cell. These spatiotemporal distribution patterns were also transformed into a more meaningful coastline-oriented coordinate system. This was done by projecting the estimated abundances in the Cartesian coordinate system onto a curvilinear axis following the coastline from Port Elizabeth on the South-African south coast to the Namibia-Angola border (Kunene River) in the North (see Fig. 1). The shortest distance to any point on the coastline, as defined in the R package "mapdata" (Becker et al. 2013), was used. The same coastline definition was used for all maps (Figure 1).

# Results

The model was fitted to the catch data and the parameter estimates are given in Table 2. The fitted model explained 67% of the variation in the data. However, it was not possible to estimate the uncertainties of the parameters using the standard approach, because of an irregularity in the likelihood surface. [***Disclaimer #3: This is the challenge we are addressing at the moment. The estimation problem mainly affects the gear selectivity. The distribution-maps are to a large extent OK, however, the overall density estimates, especially Namibia vs. South African south coast are not scaled correctly yet. We have therefore removed text and figures about the gear effect and growth. The rest is given for the user to understand the approach and get an understanding of the information that will be provided in the final peer reviewed paper***].

The resulting standard errors of the parameter are given in Table 2.

## *Gear effect*

…

## *Vital rates (Growth and Mortality)*

…

## *Spatial patterns (distribution, migration and population structure)*

The relative index of hake density (CPUE) was estimated by year and age class in each of the grid-cells throughout the study area. The hake densities were found to be spatially correlated with a spatial de-correlation distance (*H*) of 268 km. [spatial variance]. The local abundance varied substantially from haul to haul, with a CV of 70% (nugget effect). The spatial patterns of the cohorts were found to be fairly stable with a temporal de-correlation period (*T*) spanning 2.4 years. We illustrated the main trends in age-specific distributions by mapping the average spatial distributions of the seven cohorts that the model could follow from the ages of 0.5 to 7.5 years (Figure 6-7). These average distributions were then used to infer putative migrations through their life. We analysed the alongshore and the off-shore (depth) migration separately.

For scrutiny of alongshore migration patterns, we projected the distributions onto a curvilinear axis following the coastline from Port Elizabeth in the south-east to the Namibia-Angola border (Kunene River) in the North. The resulting alongshore distributions were then plotted by age for each cohort (Figure 8-9) and for the average of all cohorts (Figure 10-11). The initial distribution of the 0.5-year-old recruits, revealed five areas with high densities, separated by approximately 200 km wide areas with very low densities (Figure 6 and Figure 10). We named these nursery/recruitment areas for future reference and defined them according to the local minima that separated them (Table 3). This initial pattern was preserved well into the second year, after which, *M. capensis* began an alongshore redistribution (Figure 10-11). Substantial interannual variation in migration was observed by inspecting the cohort-specific plots (Figure 8-9). Some of the changes were so abrupt that they could only be explained as sampling noise. However, some general trends were also apparent. They stood out even more clearly on the plots of average distributions for all year classes (Figure 10-11).

From the age of 2.5 years onwards, the distribution was clearly different than the recruit distribution, showing that the recruits from Walvis, Orange and Olifants had spread out. This developed into a broad stationary patch in the Orange area, divided from a Northern migrating Walvis-patch and a southern migrating Agulhas-patch. The Walvis and Agulhas patches migrated in opposite directions away from the centre. They reached their outermost positions at the age of 3.5, after which they slowly returned. These alongshore migrations were mapped by adding the movements of the centre of gravity (CoG) onto Figure 11 (grey dashed lines). The CoG of both the Walvis component and the combined Olifants-Agulhas component moved approximately 700 km alongshore in 5 years. The alongshore migrations were combined with migrations towards deeper waters (Figure 12). At the age of 5.5, where approximately 58 % of the *M. capensis* are mature (Singh et al., 2011), the distribution reflected the nursery areas. The depth distributions differed between the areas, the further North the deeper for all ages (Figure 12). We could thus confirm the well-known offshore migration to deeper waters with age (Figure 13) and expand the understanding of the depth migration by showing systematic spatial differences.

Our results also suggest an overall shift in distribution from North to South with age (Figure 10) **[Not known before the gear selectivity issue has been solved]**. The diminishing numbers of larger fish in the North was seen in the year classes from 1998-2003, but not in 2004-2007 (Figure 8, 10, 15). It is likely the consequence of either fishing mortality and/or migration variability due to environmental factors.

The distribution maps and plots show that the border between Namibia and South Africa, presently used to separate *M. capensis* stocks, is in the middle of a high density area.

## *Abundance time series*

CPUE time series of the recruits were calculated for each area (Figure 14a). The overall annual recruitment fluctuated in the period 1998-2005, increased in 2007-2008, and remained high and stable up to 2012. The relative contributions from each of the five nursery areas to the total recruitment varied substantially from year to year through the entire time series. The average contribution in 1998-2012 was 34 % from Walvis, 24 % from Orange, 12 % from Olifants, 23 % from Agulhas and 6 % from Port Elizabeth. The CPUE time series for the 3.5 to 7.5 year old *M. capensis* indicated that most of the larger hakes were found in the Agulhas subpopulation, but in recent years this has been supplemented by increasing numbers of large hakes from the Walvis subpopulation (Figure 14c).

# Discussion

## *The GeoPop Model and its fit to the observations*

The finding of a ridge in the likelihood surface lead to some concern whether the fitting procedure had found the global optimum. The reliability of the estimates was therefore tested by selecting "true" parameters for a virtual population example. The population was then sampled and the parameters were estimated from the samples. This demonstrated that the original parameters could be re-estimated despite of the irregularity of the likelihood surface. This test was documented in Supplementary information 1.

## *Spatial patterns (distribution, migration and population structure)*

For the first time, maps and plots of the distribution and migration of *M. capensis* has been provided for the entire Benguela large marine ecosystem. Our description of the alongshore migration in South African waters is new to science. The migration of the Walvis component is generally in agreement with the results presented in Wilhelm (submitted), with a north-south migration similar to that presented here. However, we did not find any signs of an initial coastward migration of 10-15 cm fish. This coastward migration could have been missed in our annual time steps.

In our treatment of the spatial patterns, we presented annual snapshots of austral summer distributions. Seasonal migration patterns were not included. Such seasonal movements have been suggested as annually repeated inshore and off-the-bottom movement of hake for spawning in Namibian waters (Gordoa et al., 2006) as well as South African waters (Botha 1996, Millar, 2000). No direct indication of seasonal alongshore movement in concentrations of *M. capensis* have been reported for Namibian waters (Gordoa et al. 2006), this may be the case for in South African waters (Rademeyer, 2012).

The demonstrated double-sided return migration is a clear example of natal homing, but with unknown precision. Natal homing is a key component for closing the life cycles of smaller population-units by connecting the generations. This element may work towards population structuring in combination with the known spatial differences in spawning time (Jansen & et al., in prep)+ (ref to previous papers that show differences in spawning time). It is therefore reasonable to investigate the possible existence of multiple subpopulations (stocks) of *M. capensis* within the region. Genetic studies can reveal such structures, if they are persistent from generation to generation with relatively low levels of straying. The stability over time as well as the level of mixing between these subpopulations thus needs to be further analyzed and quantified. However, spatial structures that are not persistent from generation to generation will not be detected by genetic studies. Temporary sub-populations that differ in vital rates (growth and mortality) from other parts of the population may exist in certain life history phases. This should, ideally, be accounted for in stock assessments and management plans that aim at maximizing the sustainable yield (MSY).

The mentioned differences in spawning periods between North and South could be utilized in studies of natal homing and mixing. In other species, such as herring, the origin of each fish may be identified by counting daily increments on otoliths ref. We suggest that straying (mixing) of hakes from different spawning areas could be analyzed in the same way.

# Conclusion

For the first time, we combined data from multiple demersal trawl surveys from the entire distribution area to estimate gear selectivity, growth rates, mortality, spatial and temporal patterns of shallow water hake (*Merluccius capensis*). Our analyses were done with a new Latent Cohort GeoPop model – a geostatistical model (aggregated log Gaussian cox process model with correlations). This model was built with the aim of tracking the cohorts in time and space.

We followed the hake from 0.5 to 7.5 years of age, from five distinct recruitment/nursery areas, through the growth oriented juvenile phase, to the spawning areas. We provided maps and plots of the distribution and migration of *M. capensis* for the entire Benguela large marine ecosystem. This revealed unknown aspects of the depth and alongshore migration patterns and how they differ between parts of the Benguela region. The return migrations demonstrated natal homing, but with unknown precision.

Spatial population structures may only be maintained during some phases of the hake life time, with sub-population separation in some ages and mixing in others. However, natal homing is a key component for closing the life cycles of smaller population-units by connecting the generations. This element may work towards population structuring in combination with the known spatial differences in spawning time.

The spatial population structures and dynamics demonstrated herein, is a dimension of the hake population ecology that is not currently accounted for in stock assessment and management of one of the two most economically valuable fish resource in the region.

# Acknowledgements

We wish to thank the lab and field assistants from NatMirc (Namibia), DAFF (South Africa) and Norway that sampled and measures the many hakes analyzed in the present study. The sampling was funded by MFMR (Namibia), DAFF (South Africa) and Norway. Data analysis and publishing was funded by EuropeAid through the EcoFish project (CRIS Number C-222387).

# Figure legends

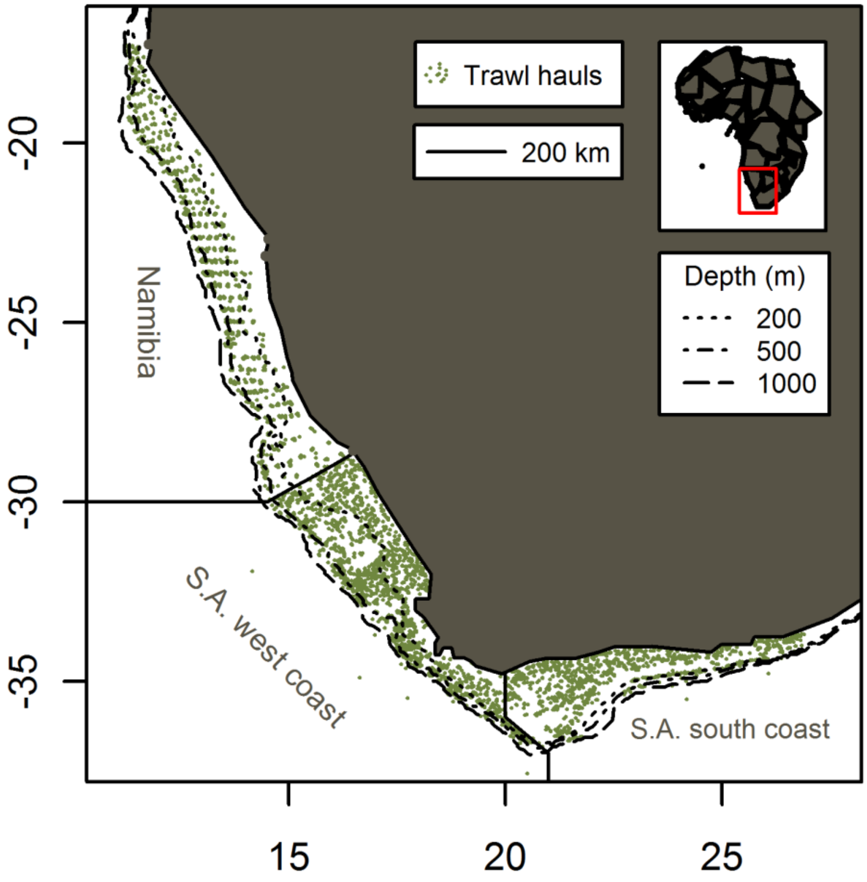

Figure 1. Map of study area with sample locations (dots), isobaths and place names referred in the text.

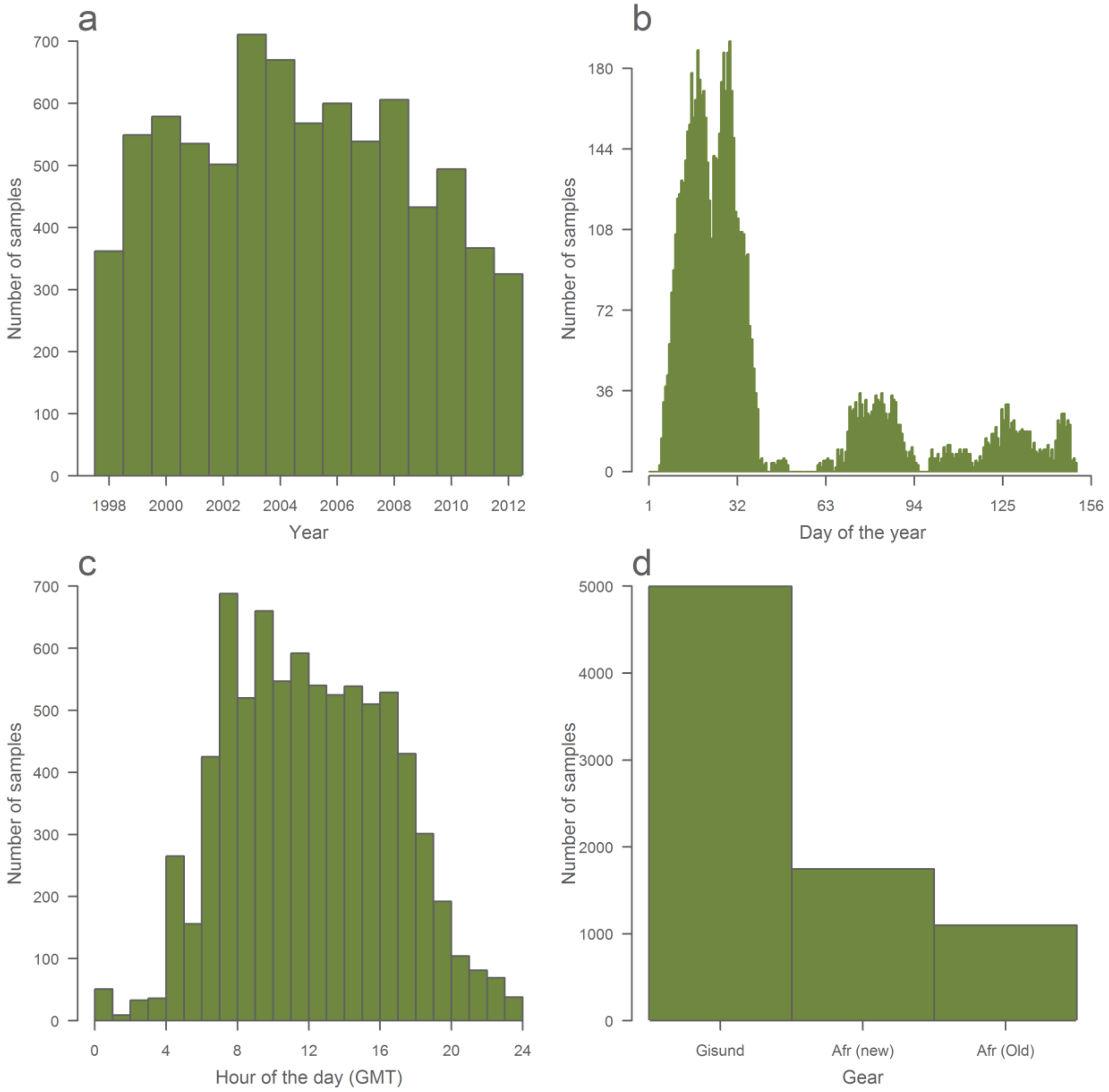

Figure 2. Bottom trawl survey samples (trawl hauls) from 1998-2012 in the studied area. Number of samples by a) year. b) ordinal day. c) hour of the day. d) gear type.

Figure 3. Estimated gear selectivity of shallow water cape hake (*M. capensis*) relative to the Gisund trawl. The grey lines and areas denote 95%-confidence intervals. Shading of the confidence interval for Afr(New) has been omitted for clarity.

Figure 4. Growth rate of shallow water cape hake (*M. capensis*). The grey areas denote the 95%-confidence interval around the estimate from the GeoPop model. Van Bertalanffy equations fitted to i) South African age readings are shown for females (upper line) and males (lower line), and ii) Namibian age reading are shown for old age readings (lower line) and new explorative age readings (upper line).

Figure 5. Total mortality of shallow water cape hake (*M. capensis*). a) Abundance by age for each year class (grey lines). Mean abundance by age (black circles). Mean abundance at the age of 0.5 years decaying with the estimated Z of 1.58 per year (black bold line). b) Total mortality by age from the present analysis (solid line) and the South African reference case stock assessment (dashed line).

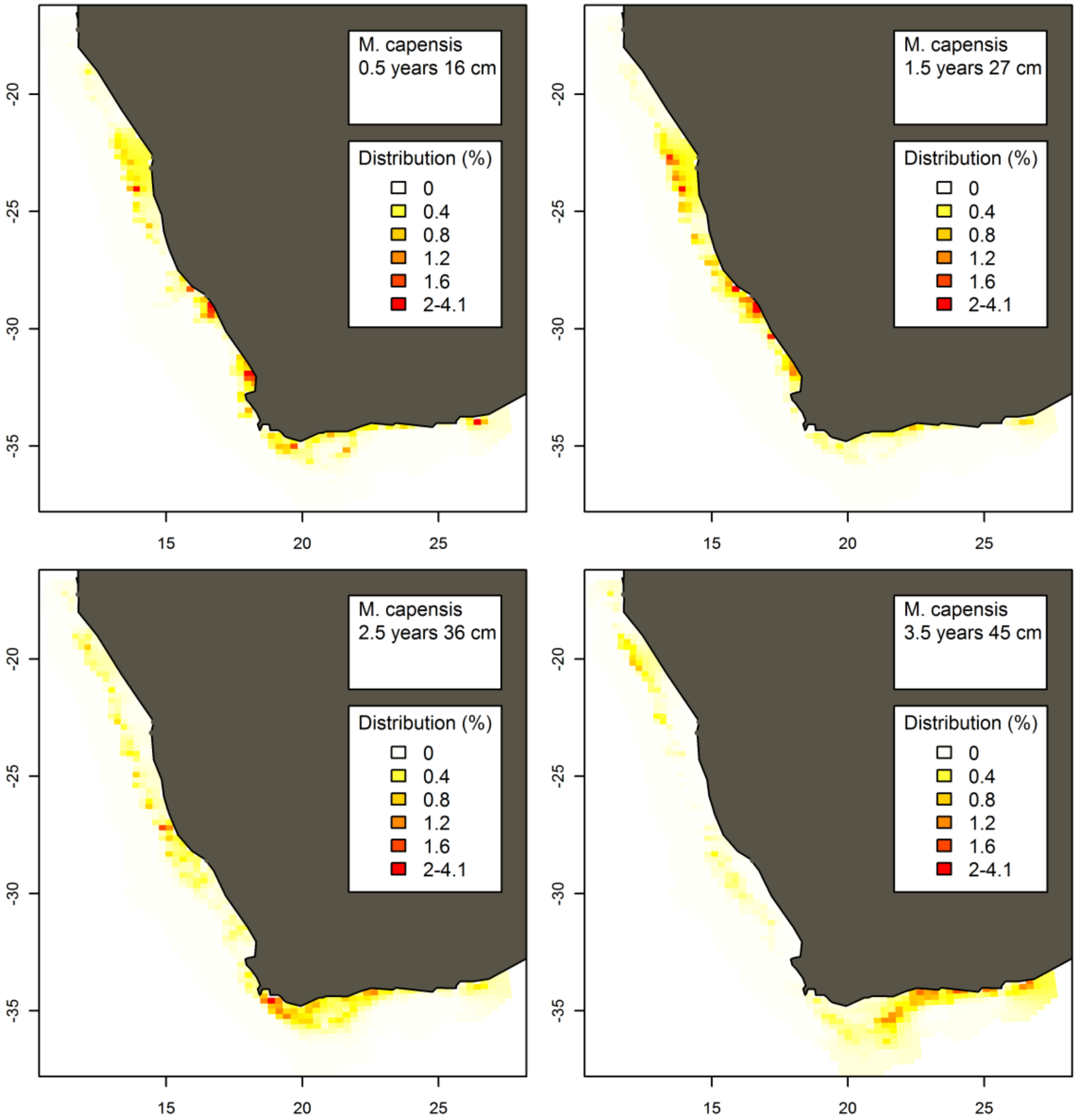

Figure 6. Distribution maps of shallow water cape hake (*M. capensis*) by age. a) 0.5 years. b) 1.5 years. c) 2.5 years. d) 3.5 years.[Bug: lengths on maps indicate length at 1, 2, 3 and 4 years of age]

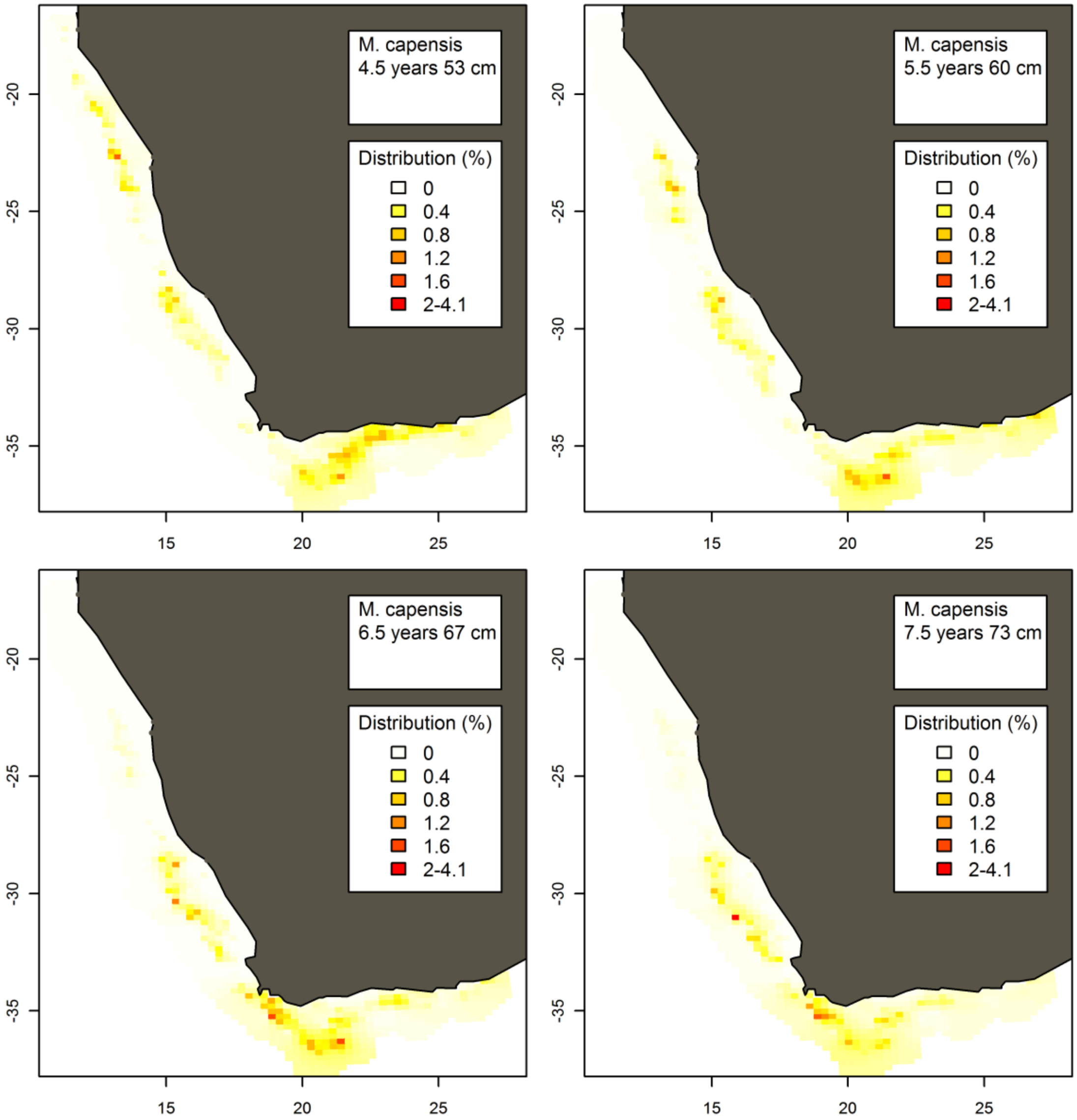

Figure 7. Distribution maps of shallow water cape hake (*M. capensis*) by age. a) 4.5 years. b) 5.5 years. c) 6.5 years. d) 7.5 years. [Bug: lengths on maps indicate length at 5, 6, 7 and 8 years of age]

Figure 8. Alongshore distribution in number of fish by age for cohorts 1998-2003 of Shallow Water Cape Hakes (*M. capensis*). The spatial distribution has been projected onto a curvilinear axis following the coastline from Port Elizabeth in the south-east to the Namibia-Angola border (Kunene River) in the North.

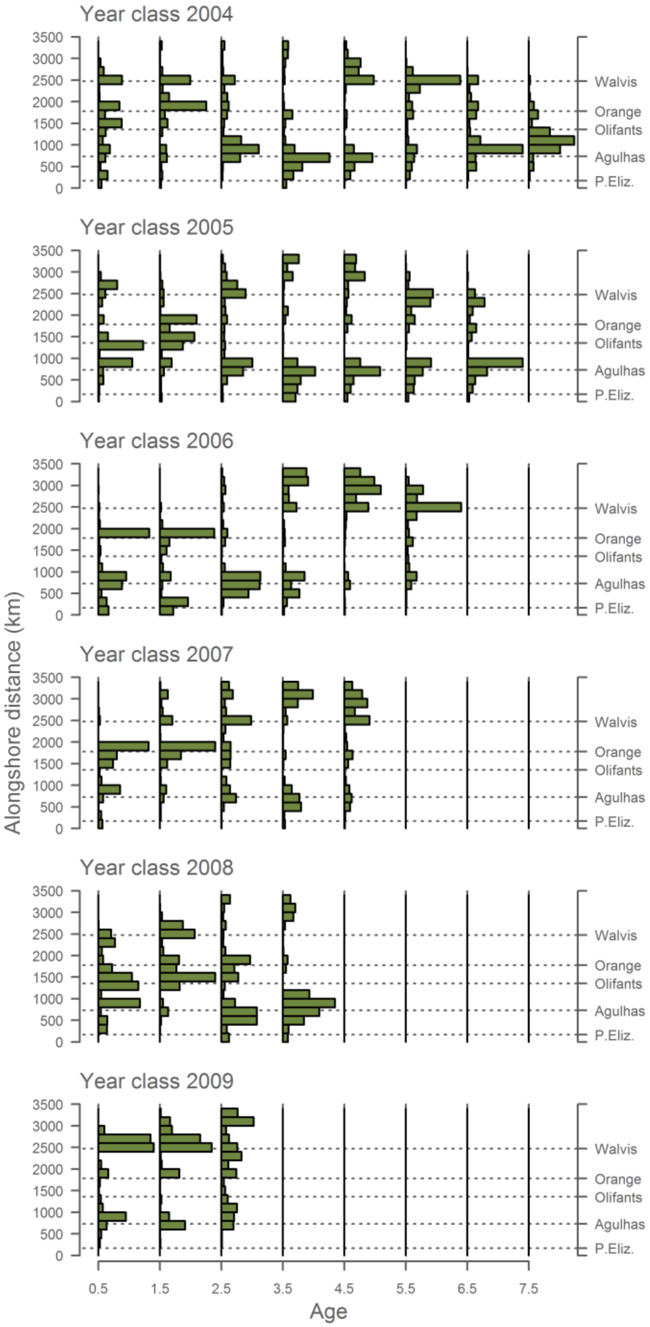

Figure 9. Alongshore distribution in number of fish by age for cohorts 2004-2009 of shallow water cape hake (*M. capensis*). The spatial distribution has been projected onto a curvilinear axis following the coastline from Port Elizabeth in the south-east to the Namibia-Angola border (Kunene River) in the North.

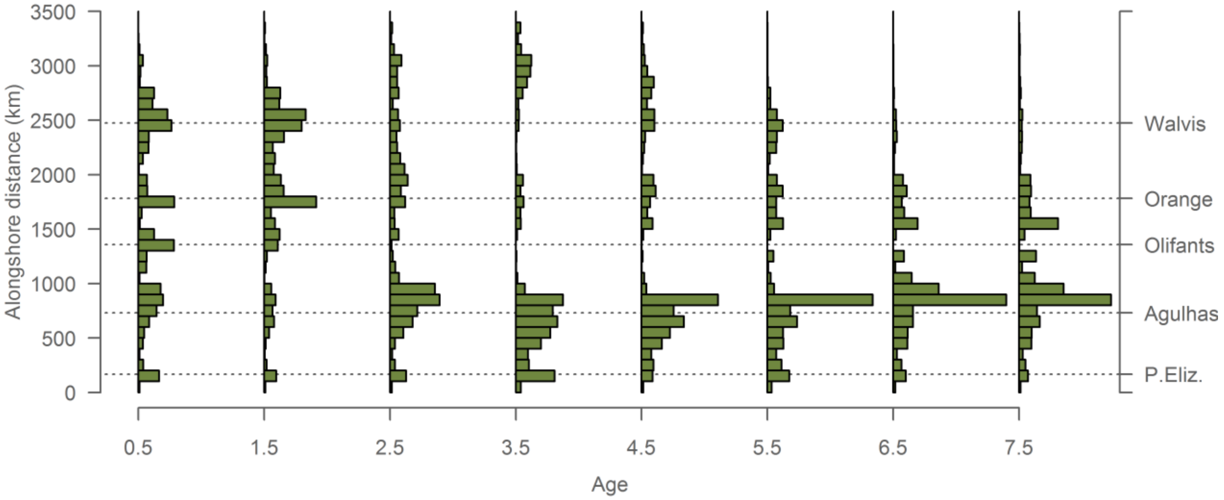

Figure 10. Alongshore distribution by age of *M. capensis*. Average of all year classes. The spatial distribution has been projected onto a curvilinear axis following the coastline from Port Elizabeth in the south-east to the Namibia-Angola border (Kunene River) in the North.

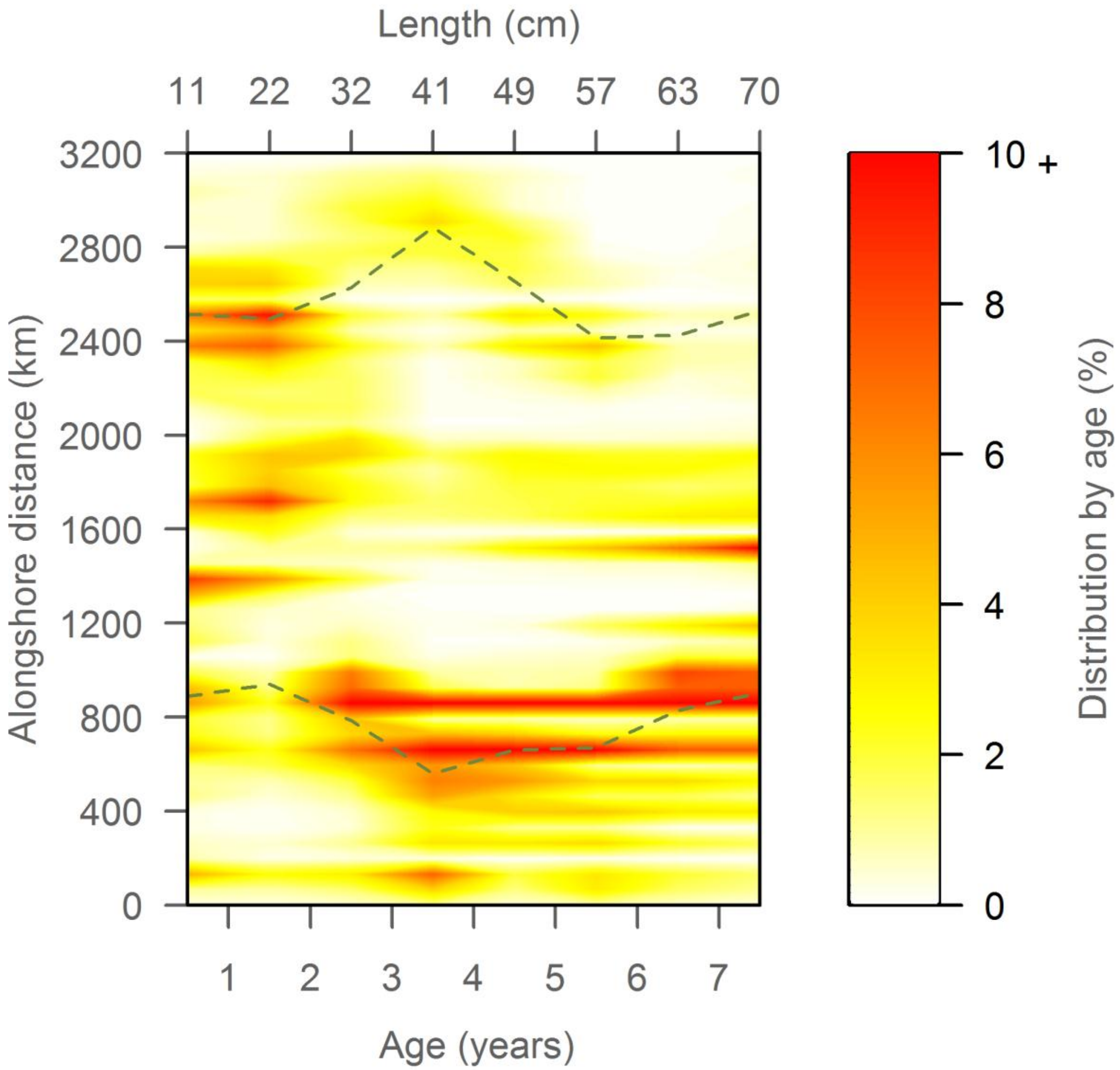

Figure 11. Alongshore distribution of *M. capensis* by age and mean length. The Centre of Gravity is indicated by grey dashed lines for hakes north of 2150 km and south of 1550 km. The spatial distribution has been projected onto a curvilinear axis following the coastline from Port Elizabeth in the south-east to the Namibia-Angola border (Kunene River) in the North.

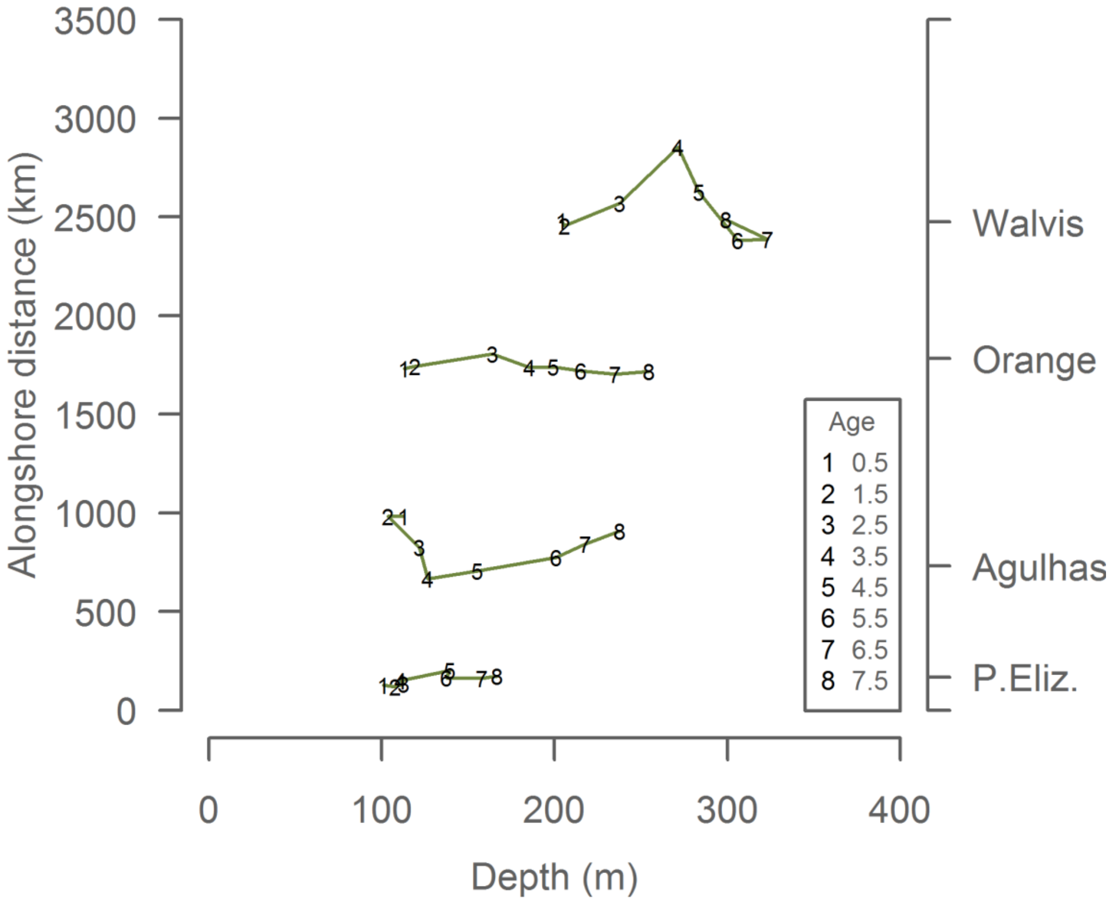

Figure 12. Centre of Gravity by age of *M. capensis* in four areas in the Benguela Current Ecosystem. Hake in the Olifants area have been included in the Agulhas area. Location names are given on the right axis.

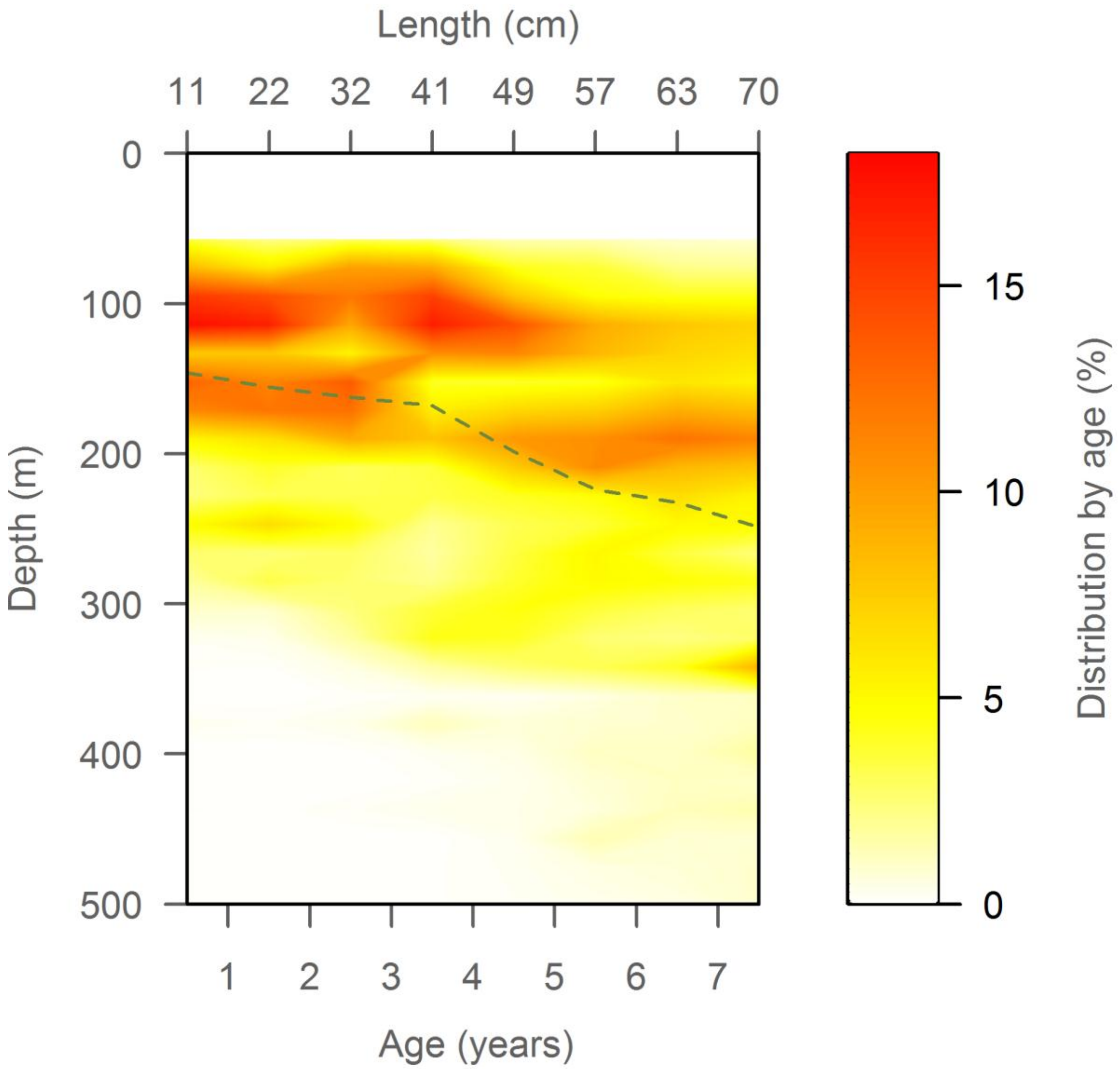

Figure 13. Depth distribution of *M. capensis* by age and mean length. Grey dashed lines indicate the mean depth.

Figure 14. Abundance index time series of *M. capensis*. a) 0.5 year old (recruits). b) 1.5-2.5 year old (juveniles). c) 3.5-7.5 year old (large juveniles and adults).

Supplementary information 1. Documentation of parameter estimation test.

Supplementary information 2. Description of the “Latent Cohort GeoPop model”.

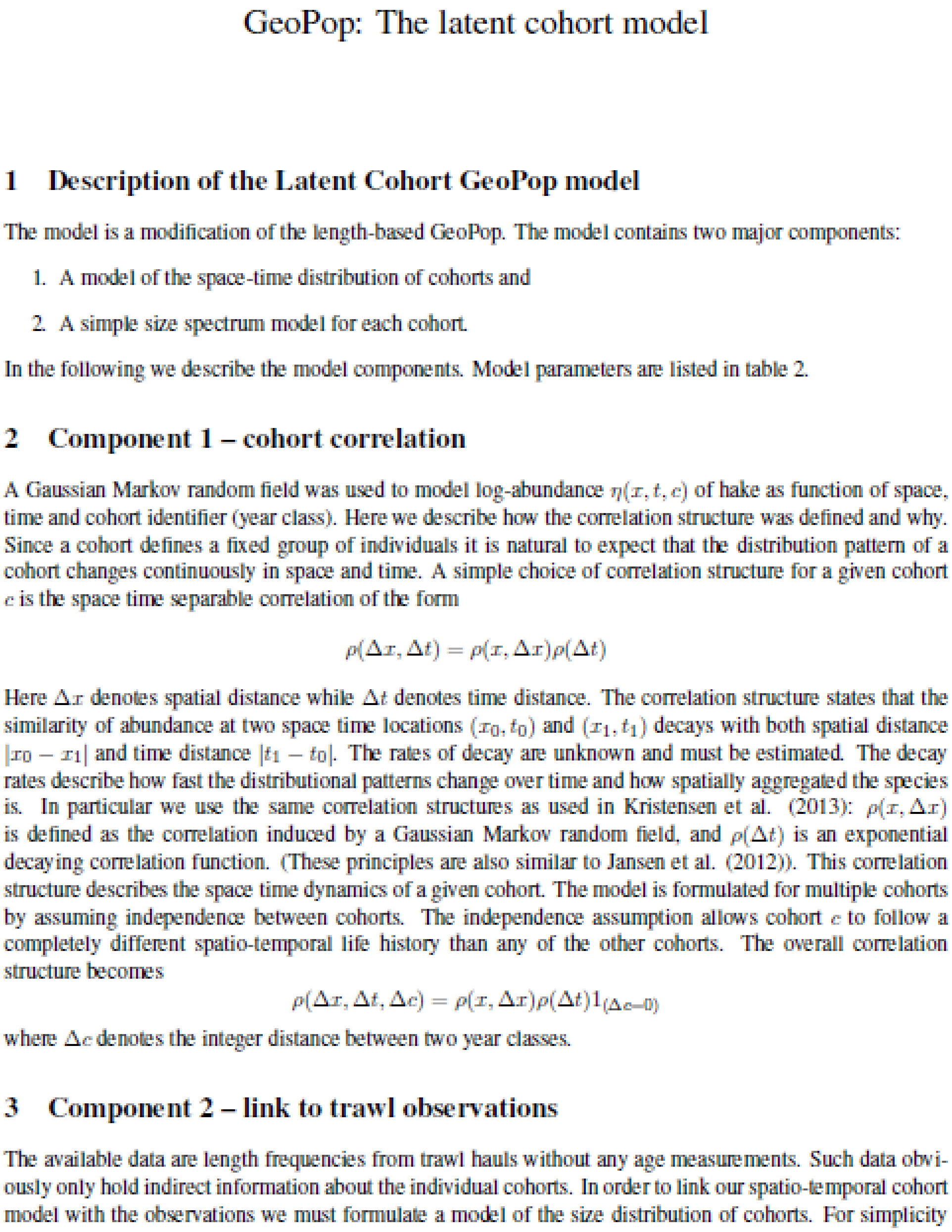

# GeoPop: The latent cohort model

## 1 Description of the Latent Cohort GeoPop model

The model is a modification of the length-based GeoPop. The model contains two major components:

1. A model of the space-time distribution of cohorts and
2. A simple size spectrum model for each cohort.

In the following we describe the model components. Model parameters are listed in table 2.

## 2 Component 1 – cohort correlation

A Gaussian Markov random field was used to model log-abundance $\eta(x,t,c)$ of hake as function of space, time and cohort identifier (year class). Here we describe how the correlation structure was defined and why. Since a cohort defines a fixed group of individuals it is natural to expect that the distribution pattern of a cohort changes continuously in space and time. A simple choice of correlation structure for a given cohort $c$ is the space time separable correlation of the form

$$\rho(\Delta x,\Delta t)=\rho(x,\Delta x)\rho(\Delta t)$$

Here $\Delta x$ denotes spatial distance while $\Delta t$ denotes time distance. The correlation structure states that the similarity of abundance at two space time locations $(x_0,t_0)$ and $(x_1,t_1)$ decays with both spatial distance $|x_0-x_1|$ and time distance $|t_1-t_0|$. The rates of decay are unknown and must be estimated. The decay rates describe how fast the distributional patterns change over time and how spatially aggregated the species is. In particular we use the same correlation structures as used in Kristensen et al. (2013): $\rho(x,\Delta x)$ is defined as the correlation induced by a Gaussian Markov random field, and $\rho(\Delta t)$ is an exponential decaying correlation function. (These principles are also similar to Jansen et al. (2012)). This correlation structure describes the space time dynamics of a given cohort. The model is formulated for multiple cohorts by assuming independence between cohorts. The independence assumption allows cohort $c$ to follow a completely different spatio-temporal life history than any of the other cohorts. The overall correlation structure becomes

$$\rho(\Delta x,\Delta t,\Delta c)=\rho(x,\Delta x)\rho(\Delta t)1_{(\Delta c=0)}$$

where $\Delta c$ denotes the integer distance between two year classes.

## 3 Component 2 – link to trawl observations

The available data are length frequencies from trawl hauls without any age measurements. Such data obviously only hold indirect information about the individual cohorts. In order to link our spatio-temporal cohort model with the observations we must formulate a model of the size distribution of cohorts. For simplicity

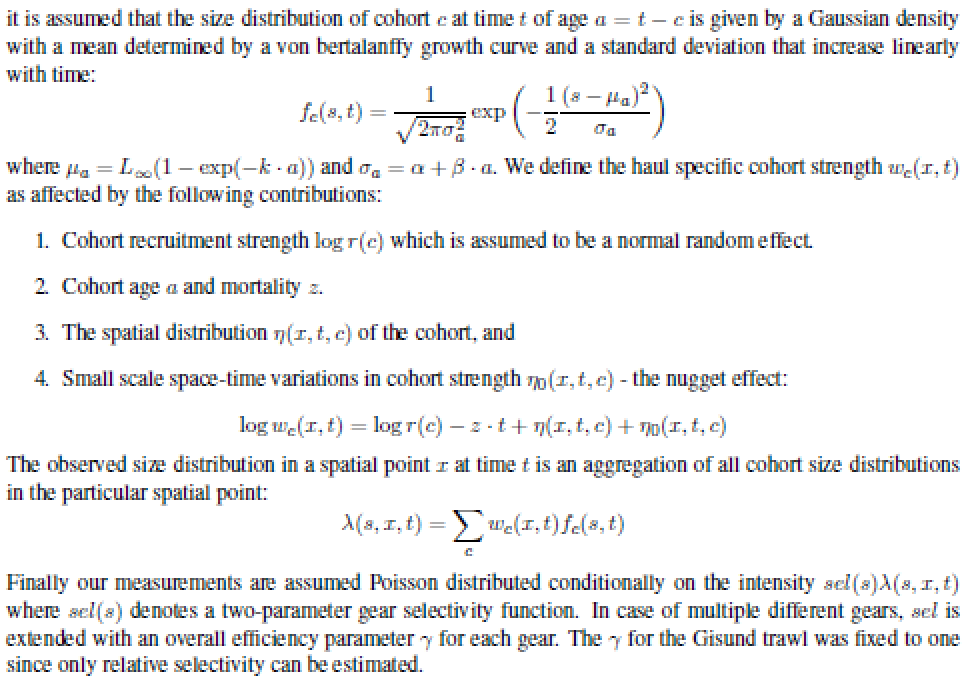

it is assumed that the size distribution of cohort $c$ at time $t$ of age $a = t - c$ is given by a Gaussian density with a mean determined by a von bertalanffy growth curve and a standard deviation that increase linearly with time:

$$f_c(s,t) = \frac{1}{\sqrt{2\pi\sigma_a^2}} \exp\left(-\frac{1}{2}\frac{(s-\mu_a)^2}{\sigma_a}\right)$$

where $\mu_a = L_\infty(1 - \exp(-k \cdot a))$ and $\sigma_a = \alpha + \beta \cdot a$. We define the haul specific cohort strength $w_c(x,t)$ as affected by the following contributions:

1. Cohort recruitment strength $\log r(c)$ which is assumed to be a normal random effect.
2. Cohort age $a$ and mortality $z$.
3. The spatial distribution $\eta(x,t,c)$ of the cohort, and
4. Small scale space-time variations in cohort strength $\eta_0(x,t,c)$ - the nugget effect:

$$\log w_c(x,t) = \log r(c) - z \cdot t + \eta(x,t,c) + \eta_0(x,t,c)$$

The observed size distribution in a spatial point $x$ at time $t$ is an aggregation of all cohort size distributions in the particular spatial point:

$$\lambda(s,x,t) = \sum_c w_c(x,t) f_c(s,t)$$

Finally our measurements are assumed Poisson distributed conditionally on the intensity $sel(s)\lambda(s,x,t)$ where $sel(s)$ denotes a two-parameter gear selectivity function. In case of multiple different gears, $sel$ is extended with an overall efficiency parameter $\gamma$ for each gear. The $\gamma$ for the Gisund trawl was fixed to one since only relative selectivity can be estimated.

# Tables

| Gear name | Standard trawl speed (knots) | Constraining rope | Door spread (m) | Sweep lengths (m) | Wing spread (m) | Headline height (m) | Mesh size in codend (mm) |
|---|---|---|---|---|---|---|---|
| Gisund | 3.0 | Yes | 50 | 40 | 21 | ? | 10 |
| Old Africana | 3.5 | No | ? | 50 | 26 | 1.7 – 4.4 | 35 |
| New Africana | 3.5 | No | ? | 9 | 24.1 – 29.2 | 2.8 – 4.8 | 35 |

Table 1. Specifications of the bottom trawl gears.

| **Symbol** | **Description** | **Unit** | **Estimate** | **Mean of estimates from bootstrap** | **Standard error** | **CV (%)** |
|---|---|---|---|---|---|---|
| $\ell_{50}^{Gisund}$ | Fish size at half selection (Gisund) | cm | … | … | … | … |
| $\ell_{50}^{SA_{New}}$ | Fish size at half selection (SA_New) | cm | … | … | … | … |
| $\ell_{50}^{SA_{Old}}$ | Fish size at half selection (SA_Old) | cm | … | … | … | … |
| $SR^{Gisund}$ | Selection range (Gisund) | cm | … | … | … | … |
| $SR^{SA\_New}$ | Selection range (SA_New) | cm | … | … | … | … |
| $SR^{SA\_Old}$ | Selection range (SA_Old) | cm | … | … | … | … |
| $\gamma_{SA_{New}}$ | Gear efficiency factor (SA_New vs. Gisund) | 1 | … | … | … | … |
| $\gamma_{SA_{Old}}$ | Gear efficiency factor (SA_Old vs. Gisund) | 1 | … | … | … | … |
| $N_0$ | Mean recruitment | #/year | … | … | … | … |
| $\sigma_{N_0}^2$ | Recruitment variance | 1 | … | … | … | … |
| $K$ | Growth rate (Von Bertalanffy) | 1/year | … | … | … | … |
| $t_0$ | Theoretical age at length 0 cm (Von Bertalanffy) | year | … | … | … | … |
| $\bar{Z}$ | Total mortality | 1/year | … | … | … | … |
| $H$ | Spatial decorrelation distance | km | … | … | … | … |
| $\sigma^2$ | Spatial variance parameter | 1 | … | … | … | … |
| $\sigma_N^2$ | Variance of the nugget effect | 1 | … | … | … | … |
| $T$ | Decorrelation time | year | … | … | … | … |

| | | | | | | |
|---|---|---|---|---|---|---|
| $\sigma^2_{init}$ | Initial length variance of cohorts | 1 | … | … | … | … |
| $\sigma^2_{rate}$ | Rate of increase in length variance of cohorts | 1/year | … | … | … | … |

Table 2. Model parameter estimates and standard errors

| **Name** | **Northern boundary (°S)** | **Southern boundary (°S)** | **Western boundary (°E)** | **Eastern boundary (°E)** |
|---|---|---|---|---|
| Walvis | NA | -27.16 | NA | NA |
| Orange | -27.16 | -31.00 | NA | NA |
| Olifants | -31.00 | -33.02 | NA | NA |
| Agulhas | -33.02 | NA | NA | 24.84 |
| Port Elizabeth | NA | NA | 24.84 | NA |

Table 3. Definitions of the spawning/retention areas. NA = Not Applicable.

# References

Agenbag, J. J. & Shannon, L. V. (1988). A suggested physical explanation for the existence of a biological boundary at 24°30'S in the Benguela system. *South African Journal of Marine Science,* 6, 119-132.

BCC (2012). Status of the Fishery Resources in the Benguela Current Large Marine Ecosystem. *, Report No. 3. Benguela Current Commission. October 2012.*

Botha, L. (1980). The biology of the Cape hake*Merluccius capensis*Cast. and*M. paradoxus*Franca. *PhD thesis, Stellenbosch University, South Africa.*

Burmeister, L. (2001). Depth-stratified density estimates and distribution of the Cape hake Merluccius capensis and M. paradoxus off Namibia, deduced from survey data, 1990–1999. *S.Afr.J.Mar.Sci., 23*, 347-356.

Duncombe-Rae, C. (2005). A demonstration of the hydrographic partition of the Benguela upwelling ecosystem at 26°40'S. *African Journal of Marine Science,* 27(3), 617-628.

Gordoa, A., & Duarte, C. M. (1991). Size-dependent spatial distribution of hake (Merluccius capensis and Merluccius paradoxus) in Namibian waters. *Can J Fish Aquat Sci, 48*, 2095-2099.

Gordoa, A., Lesch, H., & Rodergas, S. (2006). Bycatch: complementary information for understanding fish behaviour. Namibian Cape hake (M. capensis and M. paradoxus) as a case study. *ICES J Mar Sci, 63*, 1513-1519.

Jansen, T., & et al. (in prep). Spawning patterns of Shallow-water Cape hake (Merluccius capensis) shown by Gonadosomatic index (GSI). *Fish. Res.*

Jansen, T., Kristensen, K., Payne, M., Edwards, M., Schrum, C., & Pitois, S. (2012). Long-term Retrospective Analysis of Mackerel Spawning in the North Sea: A New Time Series and Modeling Approach to CPR Data. *PLoS One, 7(6)*.

Kristensen, K., Thygesen, U. H., Andersen, K. H., & Beyer, J. E. (2013). Estimating spatial-temporal dynamics of size-structured populations. *Can J Fish Aquat Sci, 99*, 1-44.

Lett, C., Veitch, J., van der Lingen, C. D. & Hutchings, L. (2007). Assessment of an environmental barrier to transport of ichthyoplankton from the southern to the northern Benguela ecosystems. *Marine Ecology Progress Series*, 347, 247-259

Lewy, P., & Kristensen, K. (2009). Modelling the distribution of fish accounting for spatial correlation and overdispersion. *Canadian Journal of Fisheries and Aquatic Sciences, 66*, 1809-1820.

MFMR, & NPC (2013). 2012 Statistics. Ministry of Fisheries and Marine Resources. www.mfmr.gov.na http://209.88.21.36/opencms/opencms/grnnet/MFMR/Fishing_Industry/statistics.html (last accessed 22 November 2013).

Payne, A. I. L. (1989). Cape hakes. *In Oceans of life off southern Africa. Ed. by A. I. L. Payne, and R. J. M. Crawford. Vlaeberg Publishers, Cape Town, South Africa*, 136-147.

Payne, A. I. L., & Punt, A. E. (1995). Biology and fisheries of South African hakes (M. capensis and M. paradoxus). *In Hake fisheries ecology and markets, pp. 15–47. Ed. by J. Alheit, and T. J. Pitcher. Chapman & Hall, London.*

Payne, A. I. L., Rose, B., & Leslie, R. W. (1987). Feeding of hake and a first attempt at determining their trophic role in the South African west coast marine environment. *African J. Mar. Sci., 5*, 471-501.

Pillar, S. C., & Wilkinson, I. S. (1995). The diet of cape hake Merluccius capensis on the south coast of South Africa. *African J. Mar. Sci., 15*, 225-239.

Rademeyer, R. A. (2012). The evolution of management procedures for the South African hake ressource in the 2000s. *PhD thesis, University of Cape Town, South Africa.*

Singh, L., Yolanda, M., & Glazer, J. (2011). Merluccius capensis and M. paradoxus length at 50% maturity based on histological analyses of gonads from surveys. *DAFF Branch Fisheries document:: FISHERIES/2011/JUL/SWG-DEM/33*.

von der Heyden, S., Lipinski, M. R., & Matthee, C. A. (2007). Mitochondrial DNA analyses of the Cape hakes reveal an expanding, panmictic population for Merluccius capensis and population structuring for mature fish in Merluccius paradoxus. *Molecular Phylogenetics and Evolution, 42*, 517-527.

Wilhelm, M. R., Jarre, A., & Moloney, C. L. (Submitted). Spawning and nursery areas, longitudinal and cross-shelf migrations of the *Merluccius capensis* stock in Namibia. *Fish. Oceanogr.*